JOURNAL OF EXPERIMENTAL AND THEORETICAL PHYSICS, 2024, Vol. 165, No. 2, pp. 283–291

STATISTICAL, NONLINEAR, AND SOFT MATTER PHYSICS

KELVIN-HELMHOLTZ INSTABILITY IN NONLINEAR OPTICS

© 2024 V.P. Ruban

Landau Institute for Theoretical Physics RAS, 142432 Chernogolovka, Moscow region, Russia

e-mail: ruban@itp.ac.ru

Received September 16, 2023

Revised October 07, 2023

Accepted October 08, 2023

Abstract. Paraxial propagation of a quasi-monochromatic light wave with two circular polarizations in a defocusing Kerr medium with anomalous dispersion inside a waveguide of annular cross-section was considered. In the phase-separated mode, the dynamics is similar to a flow of immiscible fluids. For some initial conditions with relative gliding of the fluids along the interface, the Kelvin-Helmholtz instability in its "quantum" variant is developed. Numerical simulations of the corresponding coupled nonlinear Schrodinger equations have shown formation of specific structures at the nonlinear stage of the instability. Similar structures have been known in the theory of binary Bose-Einstein condensates, but for optics they were presented for the first time.

Keywords: *nonlinear optics*, *two circular polarizations*, *defocusing Kerr medium*, *anomalous dispersion*, *coupled nonlinear Schrodinger equations*, *phase separation*

DOI: 10.31857/S00444510240214e3

1. INTRODUCTION

The study of nonlinear waves of different physical nature is, first of all, a search for possible coherent structures in a given system. Perhaps the best known are such long-lived objects as solitons and vortices (see, for example, [1-7]). Of great interest are also structures formed as a result of the development of different kinds of instabilities. A striking example is the Kelvin-Helmholtz instability (KHI), which occurs in liquid systems in the presence of a tangential discontinuity in the velocity field. A quantum analog of this instability in superfluid ^{3}He has been discovered relatively recently [8-11]. The KHI is also known for two-component ultracold gases (Bose–Einstein condensates, BEC) in the spatial phase separation regime [12-14], where it has been theoretically studied along with other analogs of classical hydrodynamic instabilities [15-20]. The example of BSCs is particularly interesting because in the zero-temperature limit these rarefied systems are well described by a rather simple and universal mathematical model – the coupled nonlinear Schrödinger equations [21-27] (in the physics of cold Bose-gases they are called the Gross-Pitaevskii equations). In a binary BEC, in addition to dark solitons and quantized vortices in each of the two components, domain walls are still possible due to the dominance of the crossed nonlinear interaction. The domain wall has an effective surface tension [24, 28, 29], which significantly participates in the interface dynamics at all stages of instability development.

The coupled nonlinear Schrödinger equations (NSE) are known to arise in the study of many physical systems. In particular, they approximate the propagation of a quasi-monochromatic light wave with two circular polarizations in an optical medium with Kerr nonlinearity [30]. A possible difference with BECs is the hyperbolic type of the three-dimensional dispersion operator in the case of normal optical dispersion. But for anomalous dispersion and defocusing nonlinearity, the paraxial optical equations are mathematically equivalent to the two coupled Gross-Pitaevskii equations in which the KHI is developed.

Moreover, when considering spatially two-dimensional solutions, as in [12-14], the type of dispersion is formally unimportant since there is no dependence on the corresponding third coordinate (unless one is interested in the dynamics of small three-dimensional perturbations).

It should be noted that in nonlinear optics domain walls separating regions with right and left circular

polarizations of light are also known [31-40], but the KHI of such interface surfaces in the presence of relative shear flow of "light fluids" has not been considered so far. It should be emphasized that we are not talking here about the primary modulation instability of spatially homogeneous two-component systems with dominant cross-repulsion [41-43], which actually leads to phase separation through the formation of domain walls, but about the possible instability of the stationary geometrical configuration of the already existing domain wall (analogous to the instability of dark solitons in one-component NSE [44, 45]). In this sense, the KHI in the system of coupled NSEs can be called secondary. The purpose of the present work is to numerically demonstrate the development of such instability in the framework of a model that approximates the paraxial propagation of a nonlinear optical wave in a sufficiently wide annular waveguide.

2. MODEL DESCRIPTION

Note at once that the distance ζ along the waveguide axis serves as the evolutionary variable instead of time t in optics, and the role of the third "spatial" coordinate is played by the "delayed" time

$$\tau = t - \zeta / v_{gr},$$

where v_{gr} is the group velocity of light in the medium at a given carrier frequency ω_0. When comparing with BECs, one should mean t instead of ζ and z instead of τ. In dimensionless variables, the nonlinear Schrödinger equations for the slow complex envelopes $A_{1,2}(x, y, \tau, \zeta)$ of the left and right circular polarizations of the light wave are of the form (see [30-38])

$$i\frac{\partial A_{1,2}}{\partial \zeta} = \left[-\frac{1}{2}\Delta + U(x,y) + \left|A_{1,2}\right|^2 + g_{12}\left|A_{2,1}\right|^2\right]A_{1,2}, \quad (1)$$

where

$$\Delta = \partial_x^2 + \partial_y^2 + \partial_\tau^2$$

is the three-dimensional Laplace operator in the "coordinate" space (x, y, τ). In the case of normal dispersion, the sign in front of ∂_τ^2 is reversed. The potential $U(x, y)$ is determined by the dielectric permittivity profile in the cross section of the waveguide. The cross-phase modulation parameter g_{12} in the typical case is approximately equal to 2, which corresponds to the phase separation mode.

We would like to remind the assumptions for the model (1). This system is derived for a weakly inhomogeneous medium in which the background dielectric permittivity is a function of frequency $\varepsilon(\omega)$, so that the corresponding dispersion law has the following form

$$k(\omega) = \sqrt{\varepsilon(\omega)}\omega / c.$$

The range of the anomalous group velocity dispersion of interest to us (where $k''(\omega) < 0$) is usually near the low-frequency edge of the transparency window (in real substances this is often the infrared region of the spectrum; see, e.g., [46-48]). It follows from Maxwell's equations that in an optical wave the electric field $\boldsymbol{E}$ and the electric induction field $\boldsymbol{D}$ are related by equation

$$\text{rot rot}\, E = -\frac{1}{c^2}\frac{\partial^2 D}{\partial t^2}.$$

Slow complex envelopes $\mathbf{E}$ and $\mathbf{D}$ are introduced by substitutions

$$\boldsymbol{E} \approx \text{Re}\left[\mathbf{E}\exp(ik_0\zeta - i\omega_0 t)\right],$$
$$\boldsymbol{D} \approx \text{Re}\left[\mathbf{D}\exp\left(ik_0\zeta - i\omega_0 t\right)\right],$$

where $k_0 = k(\omega_0)$ is the carrier wave number. We assume a weakly nonlinear material dependence of the Kerr type

$$\begin{aligned}\mathbf{D} \approx\ & \varepsilon\left(\omega_0 + i\partial_t\right)\mathbf{E} + \tilde{\varepsilon}\left(x,y\right)\mathbf{E} + \\ & + \alpha\left(\omega_0\right)\left|\mathbf{E}\right|^2\mathbf{E} + \beta\left(\omega_0\right)\left(\mathbf{E}\cdot\mathbf{E}\right)\mathbf{E}^*,\end{aligned} \quad (3)$$

with operator $\varepsilon(\omega_0 + i\partial_t)$, with spatial inhomogeneity $\tilde{\varepsilon}(x, y)$ and with negative functions α and β in the defocusing case. Substitution into (2) is then performed, with the small divergence of the electric field neglected. The linear operator $[k_0 - i\partial_\zeta]^2 - [k(\omega_0 + i\partial_t)]^2$ arising in the course of transformations is represented as a product of sum and difference, after which the expansion by powers of the operator ∂_t leads to an equation of the following form

$$2k_0\left[-i\partial_\zeta - ik_0'\partial_t + k_0''\partial_t^2/2\right]\mathbf{E} = s\{\mathbf{E}\}, \quad (4)$$

with a right-hand side that includes transverse Laplacian, nonlinearity and spatial inhomogeneity. At the end of the derivation, to pass to scalar functions $A_{1,2}$, a substitution is made to

$$\mathbf{E} \approx \left[\left(\mathbf{e}_x + i\mathbf{e}_y\right)A_1 + \left(\mathbf{e}_x - i\mathbf{e}_y\right)A_2\right] / \sqrt{2}. \quad (5)$$

The scale for the transverse coordinates is chosen to be some large parameter R_0. Let it be of the order

of several tens of wavelengths, i.e., up to one hundred micrometers. Then the width of the domain wall with the normal across the beam at the wave intensities of interest $I_{1,2} \lesssim 10$ will be at least a dozen wavelengths. The natural scale for the variable τ is the combination $k_0 R_0 \delta / \omega_0$, where the dimensionless parameter

$$\delta = \omega_0 \sqrt{|k_0''| / k_0}$$

characterizes the relative magnitude of the group velocity dispersion. Related to this combination is the condition $k_0 R_0 \delta \gg 2\pi$, which ensures quasi-monochromaticity of the wave on the variable τ. This requirement turns out to be quite onerous for small δ, but we will assume that at least $\delta \gtrsim 0.3$, and then there will be at least three wave periods per domain wall width with normal along the beam. The longitudinal coordinate ζ is measured in units of $k_0 R_0^2$ (a few centimeters), and the electric field is measured in units of

$$\frac{\sqrt{2\varepsilon(\omega_0) / |\alpha(\omega_0)|}}{k_0 R_0}.$$

The external potential then is

$$U = -\frac{k_0^2 R_0^2 \tilde{\varepsilon}}{2\varepsilon(\omega_0)}.$$

As a result, one obtains the non-dimensional equations (1), whereby

$$g_{12} = 1 + 2\frac{\beta(\omega_0)}{\alpha(\omega_0)}.$$

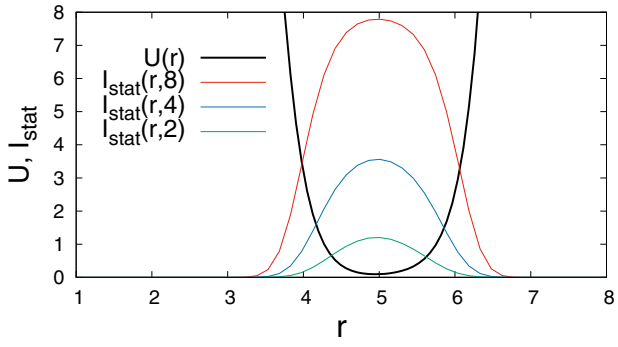

Fig. 1. A smooth potential $U(r)$ convenient for numerical modeling, roughly corresponding to an annular cross-section waveguide with a flat bottom and sharp walls. Also, equilibrium wave intensity profiles for values of the "chemical potential" $\mu = 2, 4, 8$ are shown

The well-proven split-step Fourier method for variable ζ of the second order of approximation was used for numerical modeling. As a preliminary step, unwanted hard degrees of freedom were "extinguished" by a dissipative "imaginary time propagation" procedure. The details of this approach are described in [38-40]. The computational domain had dimensions $(6\pi) \times (6\pi) \times T_\tau$, with periodic boundary conditions, and the period T_τ on the variable τ was taken equal to 24π or 48π for different numerical experiments.

3. GEOMETRY OF THE PROBLEM

Let us now turn to the geometrical characteristics of the model. In contrast to the recent work [38], where parabolic potentials were considered

$$U = \left(x^2 + \kappa^2 y^2\right) / 2,$$

here we focus on annular waveguides with the "flat" bottom and sharp walls. Such waveguides are easier to produce in practice, since the medium in them is homogeneous. But for numerical modeling by the chosen method (with a reasonable spatial grid step) only sufficiently smooth potentials are suitable. Therefore, we will approximate the corresponding deep rectangular pit only in a qualitative sense, using the following expression (see the corresponding graph in Fig. 1):

$$U(r) = 27\left[2 + \mathrm{th}\left(1.5\left(r^2/9 - 5.0\right)\right) - \mathrm{th}\left(2.4\left(r^2/9 - 1.2\right)\right)\right]. \qquad (6)$$

The large common multiplier here is taken quite arbitrarily, as long as it does not require a too small step on the variable ζ. As a result of this choice, the average waveguide radius roughly corresponds to $r = 5.0$. This value will be used in the following to visualize the wave pattern on a "median" cylindrical surface in (x, y, τ) space at different values of propagation distance ζ.

The initial conditions in our numerical experiments set the location of the domain wall approximately across the waveguide axis (its normal is approximately along the axis). In this case, the "currents" of both polarizations had an azimuthal character (with coordinate multipliers $\exp(iQ_{1,2}\phi)$, where ϕ is the azimuthal angle, Q_1 and $Q_2 \neq Q_1$ are integer "quantum" numbers). Thus, the system is three-dimensional, and hence the anomalousness of the dispersion is fundamentally important. But the difference between the outer $r + a/2$ and inner $r - a/2$ radii of the waveguide is relatively

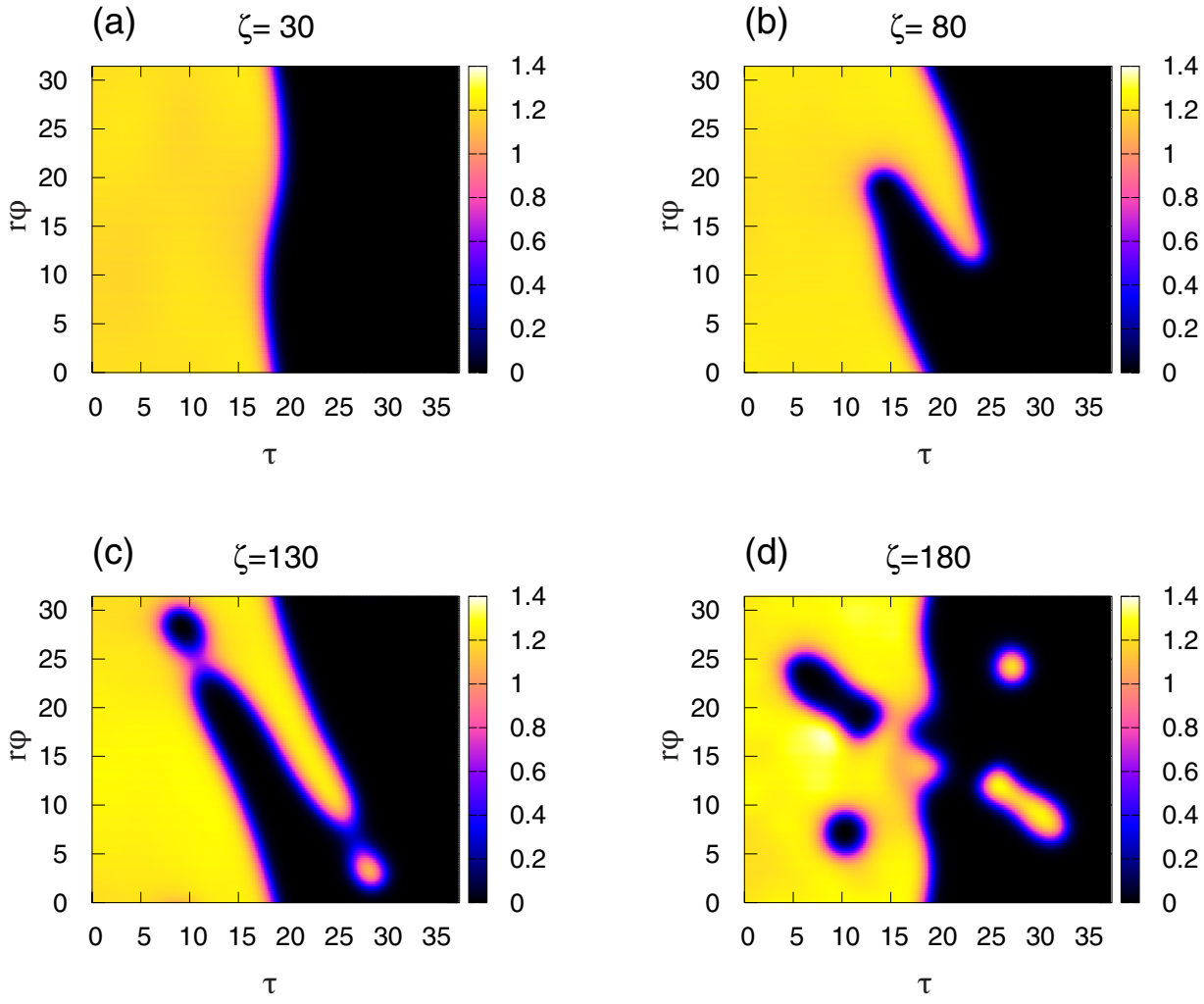

Fig. 2. Example of the development of Kelvin-Helmholtz instability at $Q = 2$ and a small level of nonlinearity $\mu = 2$. The intensity of the first component I_1 on a cylinder of radius $r = 5$ is shown for several values of the variable ζ.

small (effectively $a / r \approx 0.2$–0.4 depending on the "chemical potential" of the wave, as can be seen from the intensity profiles in Fig. 1). In such a geometry, the system behaves approximately as a spatially two-dimensional system (on a cylinder). This contributes to the manifestation of instability of the type under consideration, and is also important for the visualization of numerical results (see Fig. 2-6).

It should be noted that the system (1) also has solutions independent of τ, and there the flow occurs in the (x, y) plane. The normal to the domain wall also lies in this plane. On the one hand, these solutions are attractive because for such stationary configurations in physical space the requirement of anomalous dispersion is removed. And it is quite possible that three-dimensional perturbations would not manifest themselves at a sufficiently long propagation distance. But, on the other hand, when the transverse dimensions of the sample are finite, it becomes necessary to loop both stationary currents somehow, and then the problem of the appearance of additional transverse instabilities due to the interaction with transverse boundaries may arise. There is also a third variant of stationary flows with a shift along the contact boundary of light "liquids" – when the motion with different velocities occurs along the axis of the waveguide. This variant is described by the multipliers $\exp(i\nu_{1,2}\tau)$ and thus corresponds to some difference in the average frequency of the left and right polarizations. For this configuration, the waveguide cross-section need not be circular. The first and third options seem equally promising. In this paper, we focus on azimuthal currents.

The classical formula states that the Kelvin-Helmholtz instability increment equals

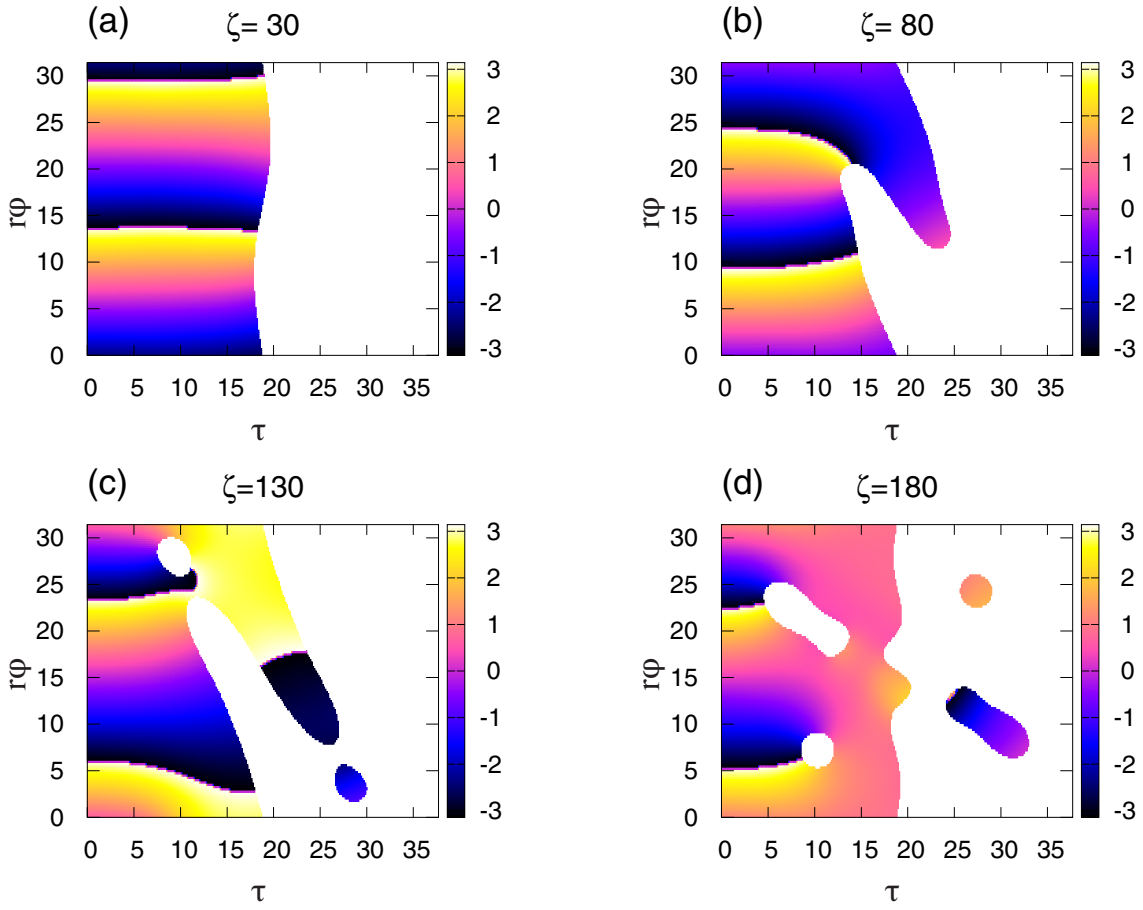

Fig. 3. Phase Θ_1 of the first components on a cylinder of radius $r = 5$, corresponding to Fig. 2. Each panel shows only that part of the cylinder involute where $I_1 > 0.4$

$$\Gamma(k) = k\sqrt{\frac{v^2}{4} - k\frac{\sigma}{2\rho}},$$

where k is the wave number, σ is the surface tension coefficient, ρ is the density of the fluid equal on both sides of the interface, v is the velocity difference for undisturbed flow. From this formula we can extract useful information for our case as well. Indeed, at sufficiently large values of the "chemical potential" μ, the density of "liquids" $\rho = I \approx \mu$, the effective surface tension coefficient of the domain wall can be estimated as $\sigma \propto \mu^{3/2}$ [28], the velocity of relative motion $v \approx (Q_1 - Q_2)/r$, and the basic wave number $k = 1/r$. As a result, we have an estimation formula

$$\Gamma \approx \frac{1}{r}\sqrt{\frac{(Q_1 - Q_2)^2}{4r^2} - C\frac{\sqrt{\mu}}{r}}, \qquad (7)$$

where C is a coefficient of the order of one. The applicability of this formula also requires that the relative velocity v is small compared to the "sound speed" of $s \sim \sqrt{\mu}$. If this condition is met, the development of instability should follow the scenario determined by the ratio of the two summands under the root sign (implying a sufficiently large longitudinal interval $T_\tau/2$ between neighboring domain walls). It follows from formula (7), in particular, that at fixed r and $(Q_1 - Q_2)$ a significant increase in the wave intensity should lead to a complete suppression of instability. This effect was indeed observed in numerical experiments. For example, with $Q_1 = -Q_2 = 2$ at $\mu = 8$ and $\mu = 10$ the instability developed, whereas at $\mu = 12$ it was already absent.

4. NUMERICAL EXAMPLES

We should be said that each stationary configuration on the variable ζ is characterized by two "chemical potentials", μ_1 and μ_2. In this case

$$A_{1,2} = \sqrt{I_{1,2}(x,y,\tau)}\exp\left(i\Theta_{1,2}(x,y,\tau) - i\mu_{1,2}\zeta\right).$$

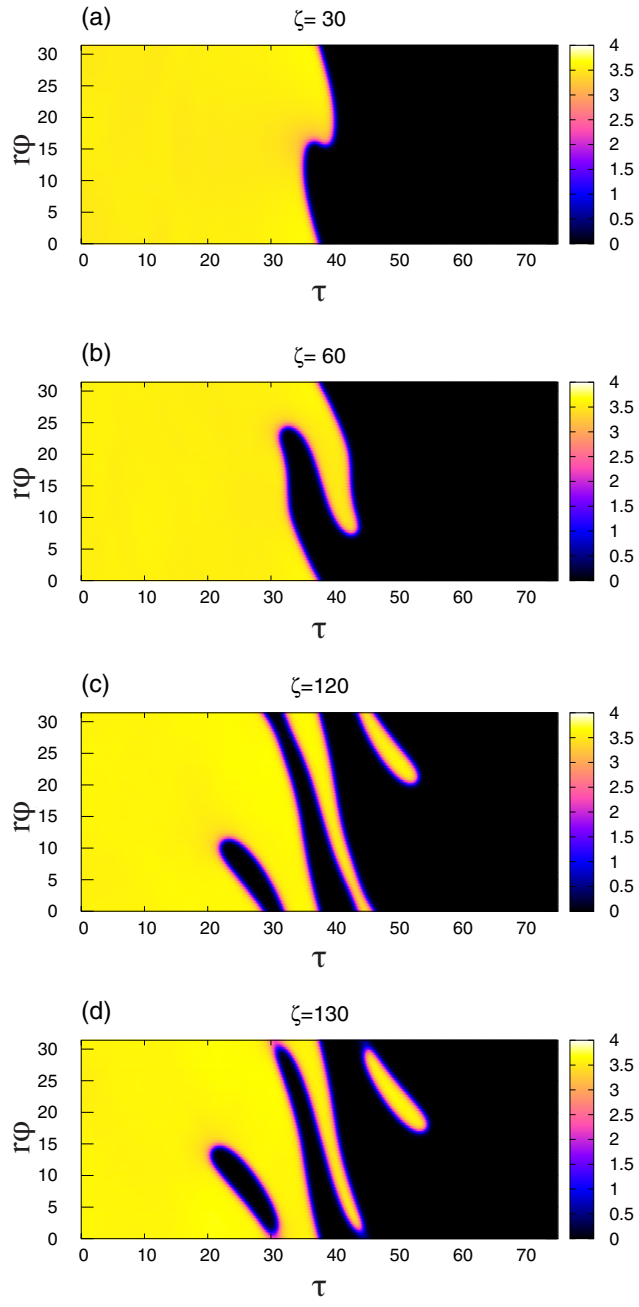

Fig. 4. Formation of long "fingers" at the intermediate stage of instability at $Q = 3$, $\mu = 4$

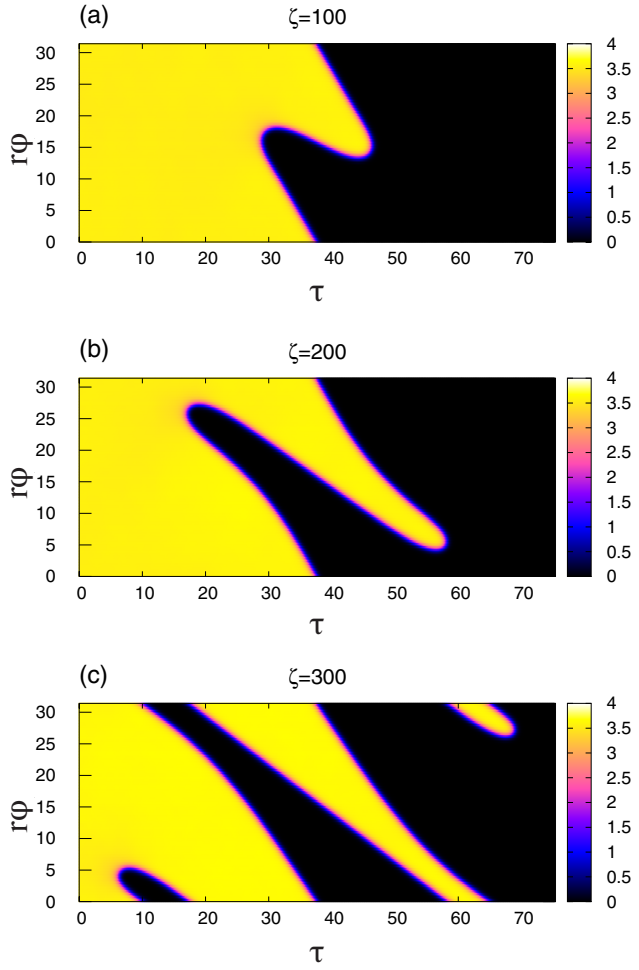

Fig. 5. Greater slope of the "fingers" at a lower relative motion velocity than in Figure 4 ($Q = 2$, $\mu = 4$)

In our case of phases $\Theta_{1,2} = Q_{1,2}\phi$. Several examples of equilibrium profiles of intensity $I_{stat}(r,\mu)$ in the presence of only one stationary component are presented in Fig. 1.

For simplicity, all numerical experiments were performed with symmetric initial conditions, so that $Q_1 = -Q_2 = Q$, and $\mu_1 = \mu_2 = \mu$. Therefore, each panel of Fig. 2-6 shows only half of the cylinder involute. In particular, Fig. 2 shows how, for $Q = 2$, $\mu = 2$, a small sinusoidal perturbation of the interface as a result of instability is transformed into a structure shaped like the silhouette of a human finger. A blob is then detached from the tip of the "finger", within which a vortex of the opposite component "sits", as follows from Fig. 3, which shows the corresponding phase distributions. Still further in each component is separated also the second similar drop. Fig. 4 demonstrates that the "finger" can extend quite a bit before it breaks and the drop separates. The angle of inclination of such "fingers" on the cylinder with respect to the azimuthal direction is greater the smaller the relative velocity (parameter Q), as can be seen by comparing Fig. 5 with Fig. 4. Finally, Fig. 6 shows that at high relative velocity ($Q = 5$) and wave intensity ($\mu = 8$) at the beginning of the nonlinear instability stage, the boundary tends to twist into a spiral structure, i.e., the instability develops according to an almost classical scenario. But

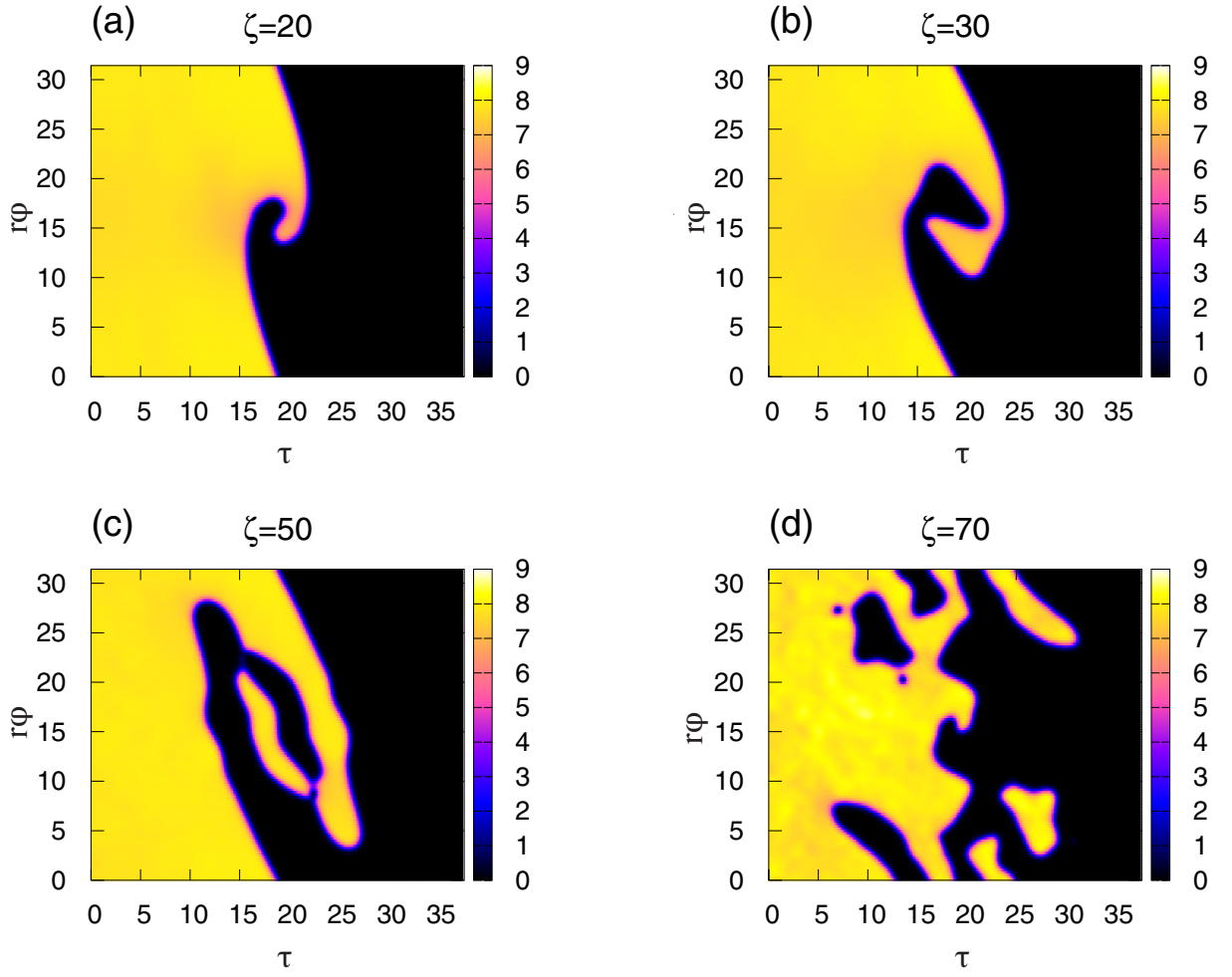

Fig. 6. Example of the development of Kelvin-Helmholtz instability with the formation of a spiral structure at the intermediate stage at $Q = 5$, $\mu = 8$

when the spatial scale of the order of the domain wall thickness $w \sim 1/\sqrt{\mu}$ reached, the dynamics switches to the "quantum" regime with the separation of drops and quantized vortices.

5. CONCLUSION

Thus, this paper theoretically substantiates the fundamental possibility of observing Kelvin-Helmholtz instability in a defocusing Kerr optical medium with the anomalous group velocity dispersion. The three-dimensional numerical simulation yielded configurations qualitatively similar to two-dimensional structures obtained in [12-14] for an idealized model of a binary BEC in unbounded space. Obviously, our three-dimensional results equally apply to BECs placed in a cylindrical confinement potential with a deep minimum at a finite value of the radial coordinate. But for cold gases such potentials remain unrealistic for the time being, whereas from the point of view of optics, there is nothing unusual in a time-length light beam propagating along a waveguide of a given cross section. From the practical point of view, the advantage of the optical structures considered here are also their not small spatial dimensions in comparison with BECs, not to mention the absence of extreme temperature constraints.

We used the simplest model, which does not take into account dispersion corrections of higher orders. In reality, the parameter δ can be so small that (at not too large values of the product $k_0 R_0$) deviations from the quadratic dispersion will have a noticeable effect. However, as shown by additional numerical experiments (their results are not presented here), taking into account the relatively small third-order dispersion, although it distorts the picture of the instability development somewhat, but does not spoil it qualitatively at a sufficiently large distance.

FUNDING

The work was carried out within the framework of the State Assignment No. 0029-2021-0003.

REFERENCES

1. Y. Kivshar and G. P. Agrawal, *Optical Solitons*: *From Fibers to Photonic Crystals*, 1st ed., Academic Press, California, USA (2003).
2. B. A. Malomed, *Multidimensional Solitons*, AIP Publishing (online), Melville, N. Y. (2022), DOI:10.1063/9780735425118
3. F. Baronio, S. Wabnitz, and Yu. Kodama, *Phys. Rev. Lett.* **116**, 173901 (2016).
4. P. G. Kevrekidis, D. J. Frantzeskakis, and R. Carretero-Gonz´alez, *The Defocusing Nonlinear Schrödinger Equation*: *From Dark Solitons to Vortices and Vortex Rings*, SIAM, Philadelphia (2015).
5. V. N. Serkin and A. Hasegawa, *JETP Lett.* **72**, 89 (2000).
6. S. K. Turitsyn, N. N. Rozanov, I. A. Yarutkina, A. E. Bednyakova, S. V. Fedorov, O. V. Shtyrina, M. P. Fedoruk, *Phys. Usp.* **59**, 642 (2016). DOI:10.3367/UFNe.2015.12.037674
7. N. A. Veretenov, N. N. Rosanov, S. V. Fedorov, *Phys. Usp.* **65** 131 (2022). DOI:10.3367/UFNe.2020.11.038869
8. R. Blaauwgeers, V. Eltsov, G. Eska, A. Finne, R. P. Haley, M. Krusius, J. Ruohio, L. Skrbek, and G. Volovik, *Phys. Rev. Lett.* **89**, 155301 (2002).
9. G.E. Volovik, Pis'ma Zh. Eksp. Teor. Fiz. 75, 491 (2002) [JETP Lett. 75, 418 (2002)].
10. A. Finne, V. Eltsov, R. H¨anninen, N. Kopnin, J. Kopu, M. Krusius, M. Tsubota, and G. Volovik, Rep. Progr. Phys. 69, 3157 (2006).
11. V. Eltsov, A. Gordeev, and M. Krusius, Phys. Rev. B 99, 054104 (2019).
12. H. Takeuchi, N. Suzuki, K. Kasamatsu, H. Saito, and M. Tsubota, Phys. Rev. B 81, 094517 (2010).
13. N. Suzuki, H. Takeuchi, K. Kasamatsu, M. Tsubota, and H. Saito, Phys. Rev. A 82, 063604 (2010).
14. H. Kokubo, K. Kasamatsu, and H. Takeuchi, Phys. Rev. A 104, 023312 (2021).
15. K. Sasaki, N. Suzuki, D. Akamatsu, and H. Saito, Phys. Rev. A 80, 063611 (2009).
16. S. Gautam and D. Angom, Phys. Rev. A 81, 053616 (2010).
17. T. Kadokura, T. Aioi, K. Sasaki, T. Kishimoto, and H. Saito, Phys. Rev. A 85, 013602 (2012).
18. K. Sasaki, N. Suzuki, and H. Saito, Phys. Rev. A 83, 053606 (2011).
19. D. Kobyakov, V. Bychkov, E. Lundh, A. Bezett, and M. Marklund, Phys. Rev. A 86, 023614 (2012).
20. D. K. Maity, K. Mukherjee, S. I. Mistakidis, S. Das, P. G. Kevrekidis, S. Ma- jumder, and P. Schmelcher, Phys. Rev. A 102, 033320 (2020).
21. Tin-Lun Ho and V. B. Shenoy, Phys. Rev. Lett. 77, 3276 (1996).
22. H. Pu and N. P. Bigelow, Phys. Rev. Lett. 80, 1130 (1998).
23. B. P. Anderson, P. C. Haljan, C. E. Wieman, and E. A. Cornell, Phys. Rev. Lett. 85, 2857 (2000).
24. S. Coen and M. Haelterman, Phys. Rev. Lett. 87, 140401 (2001).
25. G. Modugno, M. Modugno, F. Riboli, G. Roati, and M. Inguscio, Phys. Rev. Lett. 89, 190404 (2002).
26. E. Timmermans, Phys. Rev. Lett. 81, 5718 (1998).
27. P. Ao and S. T. Chui, Phys. Rev. A 58, 4836 (1998).
28. B. Van Schaeybroeck, Phys. Rev. A 78, 023624 (2008).
29. K. Sasaki, N. Suzuki, and H. Saito, Phys. Rev. A 83, 033602 (2011).
30. A. L. Berkhoer and V. E. Zakharov, Sov. Phys. JETP 31, 486 (1970).
31. M. Haelterman and A. P. Sheppard, Phys. Rev. E 49, 3389 (1994).
32. M. Haelterman and A. P. Sheppard, Phys. Rev. E 49, 4512 (1994).
33. A. P. Sheppard and M. Haelterman, Opt. Lett. 19, 859 (1994).
34. Yu. S. Kivhsar and B. Luther-Davies, Phys. Rep. 298, 81 (1998).
35. N. Dror, B. A. Malomed, and J. Zeng, Phys. Rev. E 84, 046602 (2011).
36. A. H. Carlsson, J. N. Malmberg, D. Anderson, M. Lisak, E. A. Ostrovskaya, T. J. Alexander, and Yu. S. Kivshar, Opt. Lett. 25, 660 (2000).
37. A. S. Desyatnikov, L. Torner, and Yu. S. Kivshar, Progress in Optics 47, 291 (2005).
38. V. P. Ruban, JETP Lett. 117, 292 (2023).
39. V. P. Ruban, JETP Lett. 117, 583 (2023).
40. V. P. Ruban, J. Exp. Theor. Phys. 137, 746 (2023).
41. G. P. Agrawal, Phys. Rev. Lett. 59, 880 (1987).
42. Yu. S. Kivshar and D. E. Pelinovsky, Phys. Rep. 331, 117 (2000).
43. E. E. Serebryannikov, S. O. Konorov, A. A. Ivanov, M. V. Fedorov, M. V. Alfimov, and A. M. Zheltikov, J. Exp. Theor. Phys. 102, 707 (2006).
44. E. A. Kuznetsov, S. K. Turitsyn, Sov. Phys. JETP 67, 1583 (1988).

45. V. A. Mironov, A. I. Smirnov, L. A. Smirnov, J. Exp. Theor. Phys. 112, 46 (2011).
46. X. Liu, B. Zhou, H. Guo, and M. Bache, Opt. Lett. 40, 3798 (2015).
47. X. Liu and M. Bache, Opt. Lett. 40, 4257 (2015).
48. E. D. Zaloznaya, A. E. Dormidonov, V. O. Kompanets, S. V. Chekalin, V. P. Kandidov, JETP Lett. 113, 787 (2021).